Measurement and Correlation of the Thermal Conductivity of *trans*-1-Chloro-3,3,3-trifluoropropene (R1233zd(E))†

Richard A. Perkins* and Marcia L. Huber

Applied Chemicals and Materials Division
National Institute of Standards and Technology
325 Broadway
Boulder, Colorado 80305-3337, U.S.A.

Marc J. Assael

Laboratory of Thermophysical Properties and Environmental Processes, Chemical Engineering Department, Aristotle University, Thessaloniki 54636, Greece

* Corresponding author. Email: richard.perkins@nist.gov

ABSTRACT: New experimental data on the thermal conductivity of *trans*-1-chloro-3,3,3-trifluoropropene (R1233zd(E)) are reported that allow the development of wide-range correlations. These new experimental data, covering a temperature range of 204 K to 453 K at pressures from 0.1 MPa to 67 MPa, are used to develop a correlation for the thermal conductivity. The experimental data reported here have an uncertainty of (1 - 1.5) % for liquid measurements and for gas at pressures above 1 MPa, increasing to (3 - 4) % for gas at low pressures (less than 1 MPa) and near the gas-liquid critical point. Based on the uncertainty of and comparisons with the present data, the thermal-conductivity correlation for R1233zd(E) is estimated to have a relative expanded uncertainty ranging at a 95 % confidence level from 1 % to 4 % depending on the temperature and pressure, with larger uncertainties in the critical region.

KEYWORDS: correlation; R1233zd(E); refrigerant; thermal conductivity; *trans*-1-chloro-3,3,3-trifluoropropene; transient hot wire.

1. **INTRODUCTION**

The chemical *trans*-1-chloro-3,3,3-trifluoropropene, also known as R1233zd(E), CAS 102687-65-0, is an unsaturated hydrochlorofluorocarbon that has been developed as a new foam blowing agent and also as a new refrigerant for use in chillers.[1] R1233zd(E) has been approved by the U. S. Environmental Protection Agency as a blowing agent for expanded foam insulation and a refrigerant in chillers[2] and a solvent for cleaning and as a carrier for adhesives and coatings.[3]

R1233zd(E) has a relatively short atmospheric lifetime of 26 days[4, 5] due to the presence of a carbon-carbon double bond in the molecule. This is much lower than the atmospheric lifetime of other refrigerants such as HFC-245fa[6] used in similar applications.[2] It has a global warming potential of 7 relative to carbon dioxide (whose value is 1) at an integration time horizon of 100 years (GWP_{100}),[5] again much lower than other refrigerants such as HFC-245fa[6] used in similar applications.[2] The ozone depletion potential of R1233zd(E) is 0.00024 to 0.00034.[2] R1233zd(E) has low toxicity[7, 8] and is not flammable.

Hulse et al.[1] reported limited experimental data for the critical constants, vapor pressures, saturated-liquid densities, ideal-gas heat capacities, liquid viscosities, and surface tensions of R1233zd(E). Recent work by Mondéjar et al.[9] reports additional experimental data for densities, vapor pressures and sound speeds of R1233zd(E). Based on these data, Mondéjar et al.[9] developed an accurate equation of state for R1233zd(E) that is valid at temperatures from (195 to 550) K and pressures up to 100 MPa. The equation of state of Mondéjar et al.[9] is now available in the NIST REFPROP database program,[10] and is used in the present work for analysis of the thermal conductivity measurements and as the basis for the correlation of the thermal conductivity.

In this manuscript, extensive measurements are reported for the thermal conductivity of *trans*-1-chloro-3,3,3-trifluoropropene (R1233zd(E)) in its liquid, vapor, and supercritical phases at temperatures from 204 K to 453 K with pressures up to 67 MPa. Based on these accurate experimental data, a correlation for the thermal conductivities of R1233zd(E) is developed that covers the liquid, vapor, and supercritical regions.

2. EXPERIMENTAL SECTION

2.1. Sample Material. The sample of *trans*-1-chloro-3,3,3-trifluoropropene was supplied in a 1000 cm^3 steel gas cylinder with a purity of 0.99985 mole fraction on an organic basis. The sample as received was packed under nitrogen and was degassed by eight cycles of freezing and thawing in liquid nitrogen, evacuation of vapor space, and thawing after transfer to an evacuated 1000 cm^3 stainless-steel sample cylinder. On the final pumping cycle, the initial pressure in the vapor space was 8×10^{-3} Pa. Our own analysis by gas chromatography combined with mass spectrometry and infrared spectrophotometry (carried out according to the protocols of Bruno and Svoronos [11, 12]) confirmed the purity of 0.99985 mole fraction after the sample was transferred and degassed.

The R1233zd(E) sample for these measurements was also used for measurements of the density, sound speed, and vapor pressure as reported by Mondéjar et al.[9] Since the R1233zd(E) molecule contains a carbon-carbon double bond it is possible that it can polymerize with potential release of HCl and HF. Mondéjar et al.[9] reported results of testing for thermal stability of R1233zd(E) where a sample held at a pressure of 25 MPa and a temperature of 450 K for five days showed signs of decomposition. Mondéjar et al.[9] reported that a thin layer of residue was observed in the reactor after this test and analysis of the recovered sample indicated the presence of HCl and HF. A subsequent test[9] at a pressure of 15 MPa and temperature of 450 K for five days showed no indication of decomposition. Based upon these tests, the upper temperature was limited to 453 K with sample residence time limited to 1h at pressures above 15 MPa.

2.2. Transient Measurements. The measurements of thermal conductivity at temperatures below 345 K were obtained with a transient hot-wire instrument (double-wire) that has previously been described in detail.[13] During an experiment, the platinum hot wires with a diameter of 12.7 μm functioned as both electrical heat sources and resistance thermometers to measure the temperature rise. The measurement cell consisted of a pair of hot wires of differing length operated in a differential arrangement to eliminate errors due to axial conduction. The fluid around the hot wires was contained in the concentric cylindrical region bounded by the wire and the copper vessel with an inner

diameter of 9 mm. The transient hot wires were enclosed by a copper pressure vessel that could be maintained at temperatures from 30 K to 345 K with samples in the liquid, vapor, or supercritical gas phases at pressures from near 0 MPa to 70 MPa. This measurement cell requires about 25 ml of sample. Initial cell temperatures, T_i, were determined with a standard platinum resistance thermometer (SPRT) with an expanded uncertainty of $u(T_i)$=0.005 K, and pressures, P_e, are determined with a pressure transducer with an expanded uncertainty of $u(P_e)$=7 kPa. All reported uncertainties are for a coverage factor of k=2, approximately a 95 % confidence interval.

Measurements at temperatures above 345 K were made with a small-volume (5 ml) cell with a single platinum hot wire with a diameter of 12.7 μm. The fluid was contained in the cylindrical bore of a microreactor, with an inner diameter of 8 mm, which is concentric with the hot wire that is 9.731 cm long and located along the bores central axis. The hot wire has two lead wires at each end to allow separate current and sense leads for four-wire resistance measurements. The lead wires pass through a four-wire high-pressure seal with compressed ceramic sealant. The small-volume hot-wire cell can be used at temperatures from ambient to 750 K with pressures up to 70 MPa. The microreactor is located in an aluminum isothermal cylinder with holes for platinum resistance sensors for control of temperature and measurement of temperature gradients, and for an SPRT to measure the initial cell temperature, T_i, with an expanded uncertainty of $u(T_i)$=0.005 K. The measurement cell/isothermal cylinder is in turn located within a cylindrical isothermal enclosure of aluminum with a 13 mm wall thickness, which is placed in a furnace that is controlled by the system computer at the desired temperature. An air gap between the cell/isothermal cylinder and the isothermal enclosure further reduces temperature gradients in the measurement cell. Pressures, P_e, are determined with a pressure transducer with an expanded uncertainty of $u(P_e)$=7 kPa. The single-wire cell requires additional correction for axial conduction during data analysis based on the two-dimensional analytical solution of Woodfield et al.[14]

The basic theory that describes the operation of the transient hot-wire instrument is given by Healy *et al.*[15] The hot-wire cell was designed to approximate a transient line source as closely as possible, and deviations from this model are treated as corrections to the experimental temperature rise. The ideal temperature rise ΔT_{id} is given by

$$\Delta T_{\mathrm{id}} = \frac{q}{4\pi\lambda}\left[\ln(t) + \ln\left(\frac{4a}{r_0^{\,2} C} \right) \right] = \Delta T_{\mathrm{w}} + \sum_{i=1}^{10} \delta T_i \,, \tag{1}$$

where q is the power applied per unit length, λ is the thermal conductivity of the fluid, t is the elapsed time, $a = \lambda/(\rho C_p)$ is the thermal diffusivity of the fluid, ρ is the density of the fluid, C_p is the isobaric specific heat capacity of the fluid, r_0 is the radius of the hot wire, $C = 1.781...$ is the exponential of Euler's constant, ΔT_{w} is the measured temperature rise of the wire, and δT_i are corrections[15] to account for deviations from ideal line-source conduction. During analysis, a line is fit to the linear section, from 0.1 s to 1.0 s, of the ΔT_{id} versus $\ln(t)$ data, and the thermal conductivity is obtained from the slope of this line. Both thermal conductivity and thermal diffusivity can be determined with the transient hot-wire technique as shown in Eq. 1, but only the thermal conductivity results are considered here. The experimental temperature, T_{e}, associated with the thermal conductivity is the average wire temperature over the period that was fitted to obtain the thermal conductivity.

For gas-phase measurements, two corrections[14-19] must be carefully considered. First, since the thermal diffusivity of the gas is much different from that of the wire, the correction for the wire's finite radius, and length for single wires, becomes very significant. Second, the thermal diffusivity of the dilute gas varies inversely with the pressure, so it is possible for the transient thermal wave to penetrate to the outer boundary of the gas region during an experiment at low pressures.[14-19] The preferred method to deal with such corrections is to minimize them by proper design. For instance, the correction for finite wire radius can be minimized with wires of extremely small diameter (4 to 7 μm), and penetration of the thermal wave to the outer boundary can be eliminated by use of a cell with an outer boundary of large diameter. However, such designs are often not optimal for a general-purpose instrument, where such extremely fine wires may be too fragile, and large outer dimensions may require too much of a scarce sample, particularly in the liquid phase.

The present transient hot-wire wires require careful correction for the wire's finite radius during such dilute-gas measurements. Also, the measurement duration must be selected to minimize the correction for penetration to the outer boundary due to the relatively small diameter of the concentric fluid region around each hot wire. The full heat

capacity correction[15] was applied to the present measurements. Experiments were generally limited to 1.0 s, with 250 measurements of temperature rise as a function of elapsed time relative to the onset of wire heating. Fluid convection was normally not a problem for transient experiments that were 1.0 s duration or less. For a few of the measurements at the lowest pressures, the outer boundary was encountered at elapsed times less than 1.0 s, so the maximum fit period for such experiments was further reduced to minimize the magnitude of this correction. At the lowest pressures, the thermal diffusivity is the highest and the boundary is encountered sooner.

Thermal radiative heat transfer between media at two different temperatures T_1 and T_2 increases in proportion to absolute temperature cubed, because it is proportional to $(T_1^4 - T_2^4) \approx T^3 (T_1 - T_2)$ for small temperature differences. For simplicity, the thermal radiation correction was treated as if the samples were transparent to IR radiation. This approximation is considered reasonable, since the magnitude of the radiation heat transfer was insignificant at the maximum temperatures near 452 K.

2.2. Steady-State Measurements. At very low pressures, the transient hot-wire system described above can be operated in a steady-state mode, which requires smaller corrections.[14, 20] The working equation for the steady-state mode is based on a different solution of Fourier's law, but the geometry is still that of concentric cylinders. This equation can be solved for the thermal conductivity of the fluid, λ,

$$\lambda = \frac{q \ln\left(\frac{r_2}{r_1}\right)}{2\pi(T_1 - T_2)}, \tag{2}$$

where q is the applied power per unit length, r_2 is the internal radius of the outer cylinder, r_1 is the external radius of the inner cylinder (hot wire), and $\Delta T = (T_1 - T_2)$ is the measured temperature difference between the hot wire and its surrounding cavity.

For the concentric-cylinder geometry described above, the total radial heat flow per unit length, q, remains constant and is not a function of the radial position. Assuming that the thermal conductivity is a linear function of temperature, it can be shown[20] that the measured thermal conductivity is given by $\lambda = \lambda_{T1}(1 + b_\lambda(T_1 + T_2)/2)$. Thus, the measured

thermal conductivity corresponds to the value at the mean temperature of the inner and outer cylinders,

$$\overline{T} = (T_1 + T_2)/2 . \quad (3)$$

This assumption of linear temperature dependence for the thermal conductivity is valid only for experiments with small temperature differences. The density assigned to the measured thermal conductivity is calculated from an equation of state with the temperature from Eq. 3 and the experimentally measured pressure. An assessment of corrections during steady-state hot-wire measurements is given by Roder et al.[20]

3. EXPERIMENTAL RESULTS

The complete results of the transient and steady-state measurements of the thermal conductivities of R1233zd(E) are tabulated in the Supporting Information. The range of state points covered by the present measurements is shown in Figure 1 relative to the vapor-pressure curve of R1233zd(E). The total reported measurements with the low-temperature double-wire instrument include 243 transient vapor, 112 steady-state vapor and 849 transient liquid points at temperature below 346 K with pressures up to 66.6 MPa. The total reported measurements with the high-temperature single-wire instrument include 280 transient vapor, 604 transient liquid, and 316 transient supercritical points. These higher-temperature liquid and vapor measurements range from 362 K to 423 K, while a single supercritical isotherm was measured with an average temperature of 452.0 K. Transient experiments were analyzed over the period from 0.1 s to 1.0 s. The average temperatures of the vapor isotherms were (302.9, 312.9, 322.8, 332.4, 342.4, 362.3, 382.7, 402.1, and 421.7) K. The average temperatures of the liquid isotherms were (204.5, 223.2, 242.8, 262.8, 282.5, 302.2, 302.4, 322.4, 342.4, 362.6, 383.0, 402.9, and 422.9) K. These measurements are shown in Figure 2 as a function of calculated density.

The expanded uncertainty (Type A) of the slope of the corrected transient-temperature-rise data versus ln(t) over this time range is given in the tables of transient data (Supporting Information). This expanded uncertainty (k=2) depends on both temperature-rise noise and systematic deviations from the heat-transfer model of Eq. 1 after application of all corrections. At temperatures below 345 K (double-wire cell), the expanded uncertainty ranges from approximately 3 % for the gas phase at pressures below 1 MPa to less than 1 % for the liquid phase measurements. At temperatures above 345 K (single-wire cell), the

expanded uncertainty ranges from 1.5 % for the vapor and supercritical phase measurements at pressures above 1 MPa to 3-4% for gas measurements at pressures less than 1 MPa and the supercritical isotherm near the critical density, while the uncertainty is less than 1 % for the liquid phase measurements. The uncertainty of the reported thermal conductivity is always larger than the uncertainty of the slope of the ΔT_{id} vs. ln(t), which is given as a measure of the reproducibility and internal consistency of each transient measurement.

The tables of steady-state data in the Supporting Information provide the start time and the end time for evaluation of the temperature rise, and the Rayleigh number that characterizes the level of convection during the experiment. The Rayleigh numbers during the steady-state measurements were generally less than 17,000 corresponding to a 1 % correction to the measured thermal conductivity. Measurements are generally reported for five different applied powers at each initial fluid state point to verify the absence of convection during the measurements for both transient and steady-state measurements. Reported densities, and other fluid property data required for corrections to the measured temperature rise during data analysis, are calculated with Helmholtz equation of state of Mondéjar et al.[9] for each experimental temperature and pressure associated with the measured thermal conductivity. The uncertainty of the measured initial temperature (ITS-90) is 0.005 K, and the uncertainty of the pressure is 7 kPa. The measured temperature rise and experiment temperature have expanded uncertainties of 0.020 K. The steady-state thermal conductivity data have an expanded uncertainty (i.e., a coverage factor k=2, and thus a two-standard-deviation estimate) of 3 %. All points are gas at low pressures (less than 1 MPa).

4. THERMAL CONDUCTIVITY CORRELATION

We represent the thermal conductivity λ of a pure fluid as a sum of three contributions,

$$\lambda(\rho,T) = \lambda_0(T) + \Delta\lambda_r(\rho,T) + \Delta\lambda_c(\rho,T), \tag{4}$$

where λ_0 is the dilute-gas thermal conductivity, which depends only on temperature, $\Delta\lambda_r$ is the residual thermal conductivity, and $\Delta\lambda_c$ is the enhancement of the thermal conductivity in the critical region. Both $\Delta\lambda_r$ and $\Delta\lambda_c$ are functions of temperature, T, and density, ρ, with ρ calculated with an equation of state for each experimental T and P. In this work, we use

the Helmholtz equation of state of Mondéjar et al.[9] for R1233zd(E); the equation is valid at temperatures from (195 to 550) K with pressures up to 100 MPa. The critical parameters for R1233zd(E)[9] are T_c=439.6 K, P_c=3.6237 MPa, ρ_c=480.219 kg·m^{-3}, and the molar mass is 130.4944 g·mol^{-1}.

4.1. Dilute-gas thermal conductivity. We represent the dilute-gas thermal conductivity as a polynomial in reduced temperature,

$$\lambda_0(T)/(\mathrm{W\cdot m^{-1}\cdot K^{-1}}) = \sum_{k=0}^{2} A_k (T/T_c)^k, \tag{5}$$

with coefficients A_k, where T is the temperature and T_c is the critical temperature.

4.2. Residual thermal conductivity. We used a polynomial in temperature and density to represent the background, or residual, contribution to the thermal conductivity,

$$\Delta\lambda_r(\rho,T)/(\mathrm{W\cdot m^{-1}\cdot K^{-1}}) = \sum_{i=1}^{5}\left(B_{i,1} + B_{i,2}\left(\frac{T}{T_c}\right)\right)\left(\frac{\rho}{\rho_c}\right)^i, \tag{6}$$

with coefficients $B_{i,j}$, where ρ is the density and and ρ_c is the critical density. This form has been used to represent the thermal conductivity of alkanes, such as the work of Marsh et al.[21] It also has shown to be adequate to accurately represent other fluorinated refrigerants such as R134a[22] , R125[23], and more recently hydrofluoroolefins such as R1234yf and R1234ze(E).[24]

4.3. Critical Enhancement. Olchowy and Sengers[25] developed a theoretically based, but complex, model for the thermal conductivity enhancement in the critical region. We use a simplified version of their crossover model [26],

$$\Delta\lambda_c(T,\rho)/(\mathrm{W\cdot m^{-1}\cdot K^{-1}}) = \frac{\rho C_p R_0 k_B T}{6\pi\eta\xi}\left(\Omega - \Omega_0\right), \tag{7}$$

where the heat capacity at constant pressure, $C_p(T,\rho)$, is obtained from the equation of state, k_B is Boltzmann's constant, R_0 = 1.02 is a universal constant,[27] and the viscosity, $\eta(T,\rho)$, is obtained from an extended-corresponding-states estimation method,[28] as implemented in the NIST database REFPROP;[10] the coefficients are given in the Supporting Information.

The crossover functions Ω and Ω_0 are determined by

$$\Omega = \frac{2}{\pi}\left[\left(\frac{C_p - C_V}{C_p}\right)\arctan(q_d\xi) + \frac{C_V}{C_p}(q_d\xi)\right], \tag{8}$$

$$\Omega_0 = \frac{2}{\pi}\left[1 - \exp\left(\frac{-1}{(q_d\xi)^{-1} + \frac{1}{3}\left(\frac{(q_d\xi)\rho_c}{\rho}\right)^2}\right)\right]. \tag{9}$$

The heat capacity at constant volume, $C_V(T, \rho)$, is obtained from the equation of state (EOS), and the correlation length ξ is given by

$$\xi = \xi_0\left[\frac{P_c\rho}{\Gamma\rho_c^2}\right]^{\nu/\gamma}\left[\left.\frac{\partial\rho(T,\rho)}{\partial P}\right|_T - \frac{T_R}{T}\left.\frac{\partial\rho(T_R,\rho)}{\partial P}\right|_T\right]^{\nu/\gamma}, \tag{10}$$

where the critical amplitudes Γ and ξ_0 are system-dependent and are determined by the asymptotic behavior of the equation of state in the critical region. The partial derivative $\partial\rho/\partial P|_T$ is evaluated with the equation of state at the system temperature T and at a reference temperature, T_R. For the reference temperature, we select a value where the critical enhancement is assumed to be negligible: $T_R = 1.5T_c$. The exponents $\gamma = 1.239$ and $\nu = 0.63$ are universal constants.[26] We have chosen to use values of the critical amplitudes obtained from the generalized method of Perkins et al.,[29] $\Gamma = 0.059$ and $\xi_0 = 2.13\times10^{-10}$ m. The only parameter left to be determined is the cutoff wave number q_d (or, alternatively, its inverse, q_d^{-1}). When data in the critical region are available, this parameter can be obtained by regression of data, as will be done here.

4.4. Data Fitting. In order to obtain the coefficients of the correlation (A_k for the thermal conductivity of the dilute gas in the limit of zero density, Eq. 5, the coefficients B_{ij} in Eq. 6 and the value of q_d^{-1} for the critical enhancement in Eqs. 7-10) we used the fitting program ODRPACK[30] on the complete experimental data set to obtain the coefficients in Table 1 and q_d^{-1} = 0.5980 nm. Table 2 provides values of the thermal conductivity

calculated at specific T and ρ to allow verification of computer coding of the correlation. Values of pressure shown are computed from the equation of state of Mondéjar et al.[9]

4.5. Data Deviations. The present study, comprising 2404 points in the liquid, gas, and supercritical regions from T=204 K to 454 K at pressures to 67 MPa, is the most comprehensive data set available for R1233zd(E). Figure 3 shows deviations between the data and the correlation as a function of density for the gas phase at pressures less than 1 MPa and over the temperature range 302 K to 403 K, while Figure 4 shows the deviations over the entire density range of the measurements, at pressures up to 67 MPa. Figures 5 and 6 shows deviations between the data and the correlation as a function of measured temperature and pressure, respectively. The average absolute deviation (AAD) of the gas phase points (over 302 K to 343 K) at pressures up to 1 MPa is 1.6 % for the transient measurements, and 1.7% for the steady-state measurements. We estimate the uncertainty of the correlation in this region (at a 95 % confidence level) to be less than 4 %. For the liquid phase at pressures up to 67 MPa over the temperature range 204 K to 344 K, the average absolute deviation is 0.4 %, and we estimate the uncertainty to be 1 %. For the liquid phase at higher temperatures, from 362 K to 424 K, at pressures up to 45 MPa, the AAD is 0.2 %. We estimate the uncertainty of the correlation in this region is 1 %. The correlation behaves in a physically reasonable manner over the range of applicability of the equation of state of Mondéjar et al.,[9] namely from the triple point 195.15 K to 550 K at pressure up to 100 MPa, and we feel the correlation may be safely used over this entire region although the uncertainty may be larger, rising to 5% in regions where no data were available. The uncertainty in the critical region is also larger.

5. CONCLUSIONS

A total of 2404 points are reported for the thermal conductivity of R1233zd(E) in the liquid, gas, and supercritical regions at pressures to 67 MPa. The experimental data reported here have an expanded uncertainty at a 95 % confidence level of less than 1 % for liquid measurements and 3 % for gas at low pressures (less than 1 MPa), with larger uncertainties in the critical region. Based on these measurements, a correlation is developed for the thermal conductivity surface of R1233zd(E) covering the liquid, gas, and

supercritical regions that may be used from the triple point to 550 K and pressures up to 100 MPa.

■ ASSOCIATED CONTENT

Supporting Information

Tabulated experimental values (59 pages) are reported. This material is available free of charge via the Internet at http://pubs.acs.org. Also included are coefficients for the extended corresponding-states viscosity correlation.

■ AUTHOR INFORMATION

Corresponding Author

* E-mail: richard.perkins@nist.gov. Tel.: +1-303-497-5499. Fax: +1-303-497-6682

Notes

The authors declare no competing financial interest.

■ ACKNOWLEDGEMENTS

We thank Ryan Hulse and Rajiv Singh of Honeywell for providing the high-purity sample of R1233zd(E). We thank our NIST colleague Mark McLinden for valuable discussions on sample stability and for sample preparation and degassing of the sample. We thank Tom Bruno and Tara Lovestead of NIST for the chemical analysis of the sample.

■ DEDICATION

We thank the JCED Editors for organizing this Memorial Issue for Prof. Kenneth N. Marsh and are honored to contribute this manuscript. Above all we wish to express our appreciation for many collegial discussions, scientific collaborations, and valued friendship with Ken Marsh through the years. His contributions to the knowledge of

thermophysical properties as a creative researcher, his steadfast belief that no data should be reported without its associated uncertainty, and his skilled editorial work on several books and this Journal will continue to inspire and guide researchers in thermophysical properties for years to come. Thanks Ken.

■ REFERENCES

1. Hulse, R. J.; Basu, R. S.; Singh, R. R.; Thomas, R. H. P., Physical Properties of HCFO-1233zd(E). *J. Chem. Eng. Data* **2012,** 57, 3581-3586.
2. Protection of Stratospheric Ozone: Determination 27 for Significant New Alternatives Policy Program. In Federal Register, Vol. 77, No. 155, 47768-47779: 40 CFR Part 82, [EPA-HQ-OAR-2003-0118; FRL-9712-4], RIN 2060-AG12, August 10, 2012.
3. Protection of Stratospheric Ozone: Determination 28 for Significant New Alternatives Policy Program. In Federal Register, Vol. 78, No. 96: 40 CFR Part 82, [EPA-HQ-OAR-2003-0118; FRL-9813-6], May 17, 2013.
4. Sulbaek Andersen, M. P.; Nilsson, E. J. K.; Nielsen, O. J.; Johnson, M. S.; Hurley, M. D.; Wallington, T. J., Atmospheric Chemistry of trans-CF_3CH=CHCl: Kinetics of the Gas-Phase Reactions with Cl Atoms, OH Radicals, and O_3. *J. Photochem. Photobiol. A* **2008,** 199, 92-97.
5. Orkin, V. L.; Martynova, L. E.; Kurylo, M. J., Photochemical Properties of trans-1-chloro-3,3,3-trifluoropropene (trans-CHCl=$CHCF_3$): OH Reaction Rate Constant, UV and IR Absorption Spectra, Global Warming Potential, and Ozone Depletion Potential. *J. Phys. Chem. A* **2014,** 118, 5263-5271.
6. Orkin, V. L.; Huie, R. E.; Kurylo, M. J., Atmospheric Lifetimes of HFC-143a and HFC-245fa: Flash Photolysis Resonance Fluorescence Measurements of the OH Reaction Rate Constants. *J. Phys. Chem.* **1996,** 100, 8907-8912.
7. Schmidt, T.; Bertermann, R.; Rusch, G. M.; Tveit, A.; Dekant, W., Biotransformation of trans-1-chloro-3,3,3-trifluoropropene (trans-HFCO-1233ze). *Toxicol. Appl. Pharmacol.* **2013,** 268, 343-351.
8. Tveit, A.; Rusch, G. M.; Muijser, H.; van den Hoven, M. J. W.; Hoffman, G. M., The acute, genetic, developmental and inhalation toxicology of trans-1-chloro-3,3,3-trifluoropropene (HCFC-1233zd(E)). *Drug Chem. Toxicol.* **2014,** 37, 83-92.
9. Mondéjar, M. E.; McLinden, M. O.; Lemmon, E. W., Thermodynamic properties of trans-1-chloro-3,3,3-trifluoropropene (R1233zd(E): Vapor pressure, (p,ρ,T) behavior, and speed of sound measurements, and equation of state. *J. Chem. Eng. Data* **2015,** 60, 2477-2489.
10. Lemmon, E. W.; Huber, M. L.; McLinden, M. O. *NIST Standard Reference Database 23, NIST Reference Fluid Thermodynamic and Transport Properties Database (REFPROP): Version 9.1*, Standard Reference Data Program, National Institute of Standards and Technology: Gaithersburg, MD, 2013.
11. Bruno, T. J.; Svoronos, P. D. N., *CRC Handbook of Basic Tables for Chemical Analysis, 3rd Ed.* Taylor and Francis CRC Press: Boca Raton, FL, 2011.
12. Bruno, T. J.; Svoronos, P. D. N., *CRC Handbook of Fundamental Spectroscopic Correlation Charts*. Taylor and Francis CRC Press: Boca Raton, FL, 2005.
13. Roder, H. M., A Transient Hot Wire Thermal Conductivity Apparatus for Fluids. *J. Res. Natl. Bur. Stand.* **1981,** 86, 457-493.
14. Woodfield, P. L.; Fukai, J.; Fujii, M.; Takata, Y.; Shinzato, K., A Two-Dimensional Analytical Solution for the Transient Short-Hot-Wire Method. *Int. J. Thermophys.* **2008,** 29, 1278-1298.
15. Healy, J. J.; DeGroot, J. J.; Kestin, J., The Theory of the Transient Hot-Wire Method for Measuring the Thermal Conductivity. *Physica* **1976,** 82C, 392-408.

16. Assael, M. J.; Karagiannidis, L.; Richardson, S. M.; Wakeham, W. A., Compression Work using the Transient Hot-Wire Method. *Int. J. Thermophys.* **1992,** 13, 223-235.
17. Taxis, B.; Stephan, K., Application of the transient hot-wire method to gases at low pressures. *Int. J. Thermophys.* **1994,** 15, 141-153.
18. Li, S. F. Y.; Papadaki, M.; Wakeham, W. A., The measurement of the Thermal Conductivity of Gases at Low Density by the Transient Hot-Wire Technique. *High Temp. High Press.* **1993,** 25, 451-458.
19. Li, S. F. Y.; Papadaki, M.; Wakeham, W. A., Thermal Conductivity of Low-Density Polyatomic Gases. In *Thermal Conductivity 22*, Tong, T. W., Ed. Technomic Publishing: Lancaster, PA, 1994; pp 531-542.
20. Roder, H. M.; Perkins, R. A.; Laesecke, A.; Nieto de Castro, C. A., Absolute steady-state thermal conductivity measurements by use of a transient hot-wire system. *J. Res. Natl. Inst. Stand. Technol.* **2000,** 105, 221-253.
21. Marsh, K.N.; Perkins, R. A.; Ramires, M. L. V., Measurement and Correlation of the Thermal Conductivity of Propane from 86 to 600 K at Pressures to 70 MPa. *J. Chem. Eng. Data* **2002,** 47, 932-940.
22. Perkins, R. A., Laesecke, A., Howley, J., Ramires, M.L.V., Gurova, A.N. and Cusco, L. *Experimental Thermal Conductivity Values for the IUPAC Round-robin Sample of 1,1,1,2-Tetrafluoroethane (R134a)*; National Institute of Standards and Technology NISTIR 6605: 2000; p 150.
23. Perkins, R. A.; Huber, M. L., Measurement and correlation of the thermal conductivity of pentafluoroethane (R125) from 190 K to 512 K at pressures to 70 MPa. *J. Chem. Eng. Data* **2006,** 51, 898-904.
24. Perkins, R. A.; Huber, M. L., Measurement and correlation of the thermal conductivity of 2,3,3,3-tetrafluoroprop-1-ene (R1234yf) and trans-1,3,3,3-tetrafluoropropene (R1234zd(E). *J. Chem. Eng. Data* **2011,** 56, 4868-4874.
25. Olchowy, G. A.; Sengers, J. V., Crossover from Regular to Singular Behavior of the Transport Properties of Fluids in the Critical Region. *Phys. Rev. Lett.* **1988,** 61, 15-18.
26. Olchowy, G. A.; Sengers, J. V., A Simplified Representation for the Thermal Conductivity of Fluids in the Critical Region. *Int. J. Thermophys.* **1989,** 10, 417-426.
27. Krauss, R.; Weiss, V. C.; Edison, T. A.; Sengers, J. V.; Stephan, K., Transport Properties of 1,1-Difluoroethane (R152a). *Int. J. Thermophys.* **1996,** 17, 731-757.
28. Huber, M. L., Ely, J.F., A Predictive Extended Corresponding States Model for Pure and Mixed Refrigerants Including an Equation of State for R134a. *Int. J. Refrig.* **1994,** 17, 18-31.
29. Perkins, R. A.; Sengers, J. V.; Abdulagatov, I. M.; Huber, M. L., Simplified model for the critical thermal-conductivity enhancement in molecular fluids. *Int. J. Thermophys.* **2013,** 34, 191-212.
30. Boggs, P. T., Byrd, R.H., Rogers, J.E., Schnabel, R.B. *ODRPACK, Software for Orthogonal Distance Regression*; NISTIR 4834; National Institute of Standards and Technology: Gaithersburg, MD USA, 1992.

Table 1. Parameters for the dilute-gas and residual thermal conductivity of Eqs. 5 and 6 for R1233zd(E).

Dilute-Gas Thermal Conductivity of Eq 5		
k		A_k / (W·m^{-1}·K^{-1})
0		-0.140033×10^{-1}
1		0.378160×10^{-1}
2		-0.245832×10^{-2}
Residual Thermal Conductivity of Eq 6		
i	j	B_{ij} / (W·m^{-1}·K^{-1})
1	1	0.862816×10^{-2}
1	2	0.914709×10^{-3}
2	1	-0.208988×10^{-1}
2	2	-0.407914×10^{-2}
3	1	0.511968×10^{-1}
3	2	0.845668×10^{-2}
4	1	-0.349076×10^{-1}
4	2	-0.108985×10^{-1}
5	1	0.975727×10^{-2}
5	2	0.538262×10^{-2}
6	1	-0.926484×10^{-3}
6	2	-0.806009×10^{-3}

Table 2. Values of thermal conductivity calculated for R1233zd(E) with the correlation (Eq. 4 to 10) at specified T and ρ, with the coefficients in Table 1. The value of viscosity used for T=445 K and ρ =168.52 kg·m^{-3} is 19.053 μPa·s, calculated with the method described in the Supporting Information.

T / K	p / MPa*	ρ / (kg·m^{-3})	λ / (W·m^{-1}·K^{-1})
300.0	0.00	0.00	0.010659
300.0	0.10	5.4411	0.010766
300.0	20.01	1308.8	0.091399
445.0	0.00	0.00	0.021758
445.0	3.00	168.52	0.026141
445.0	3.00	168.52	0.023992**

* Pressures calculated with the equation of state of Mondéjar et al.[9] **Calculated with critical enhancement = 0.

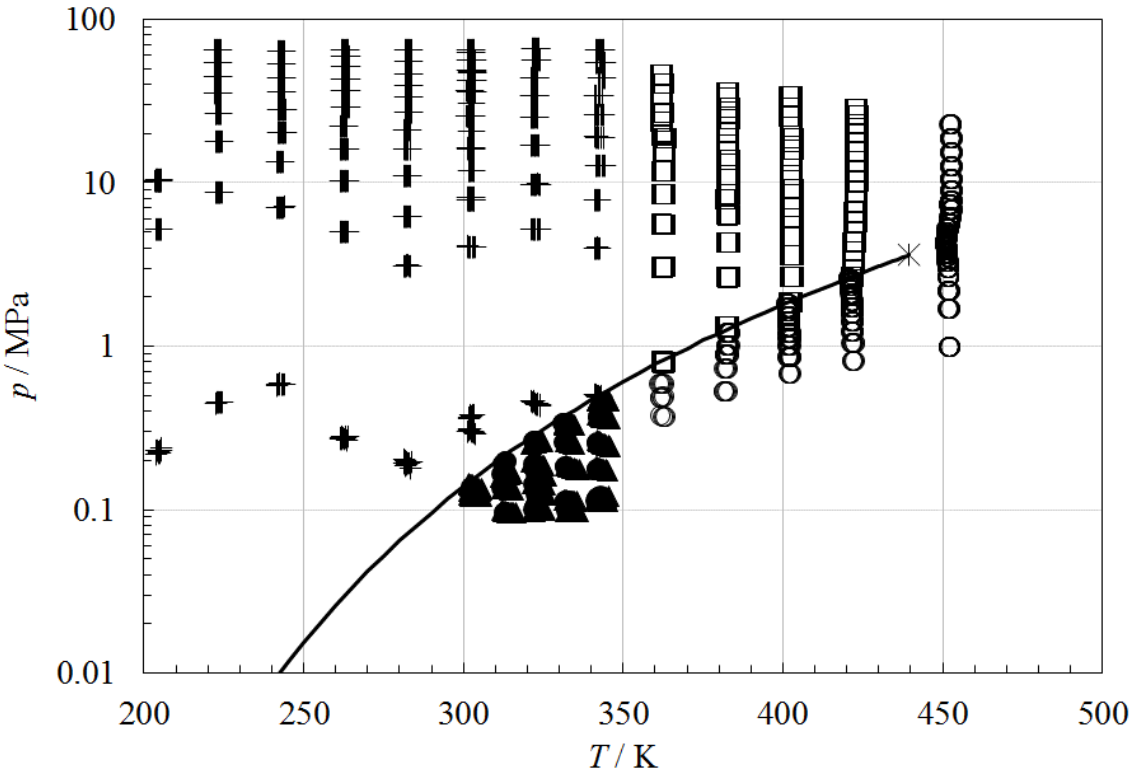

Figure 1. Distribution of the data for the thermal conductivity of R1233zd(E): ▲, double-wire transient vapor; ●, double-wire steady-state vapor; +, double-wire transient liquid; ○, single-wire transient vapor and supercritical; □, single-wire transient liquid. The solid line shows the vapor-liquid saturation boundary, terminating at the critical point, ✳ .

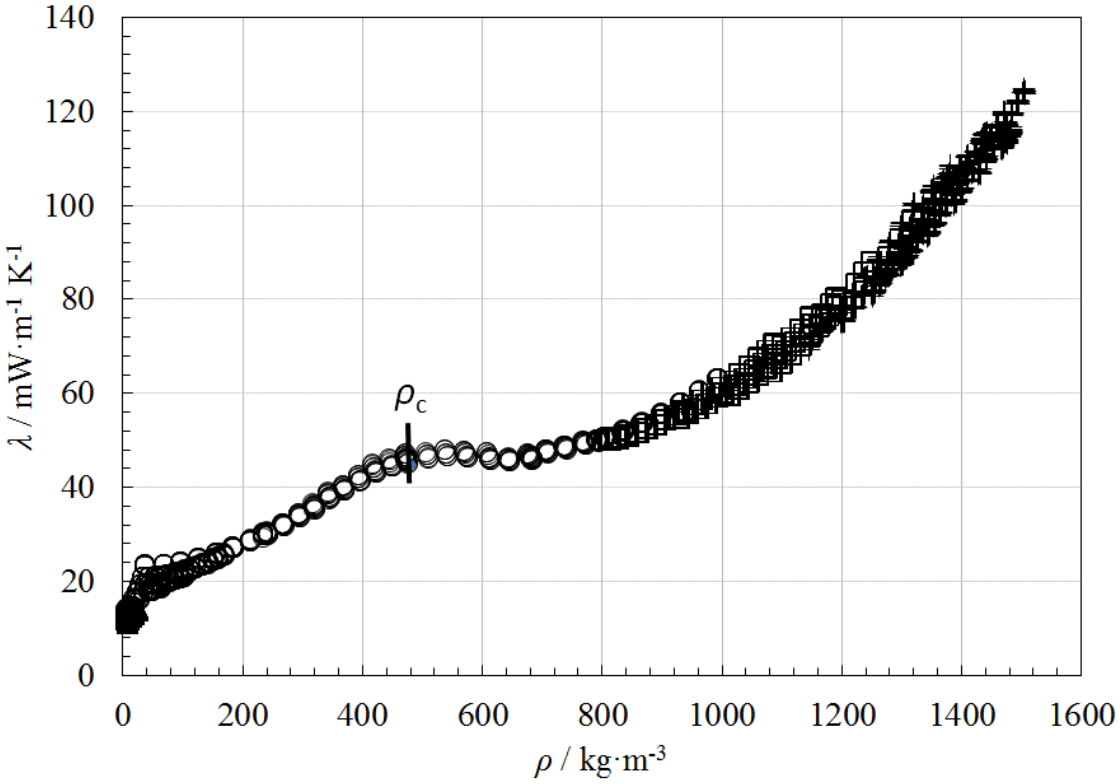

Figure 2. Thermal conductivity of R1233zd(E) as a function of the density calculated at the measured temperature and pressure: ▲, double-wire transient vapor; ●, double-wire steady-state vapor; +, double-wire transient liquid; ○, single-wire transient vapor and supercritical; □, single-wire transient liquid.

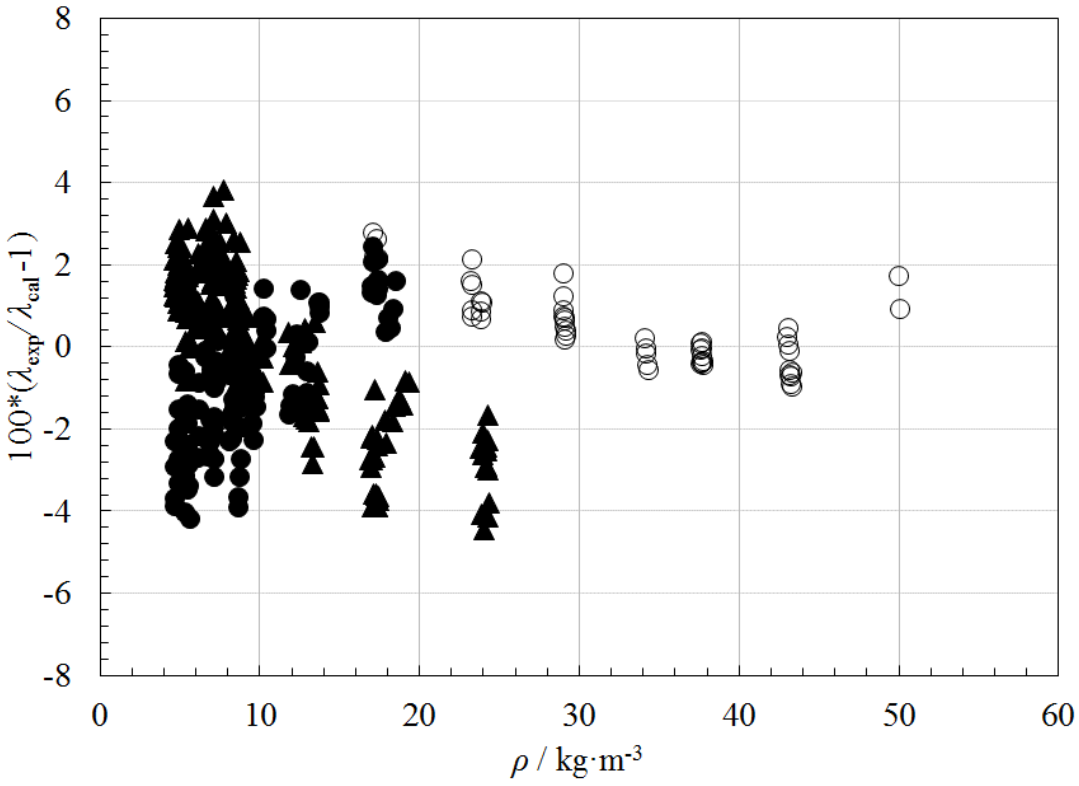

Figure 3. Relative deviation between the present experimental data (▲, double-wire transient vapor; ●, double-wire steady-state vapor; ○, single-wire transient vapor and supercritical) and the correlation for the thermal conductivity of R1233zd(E) as a function of density for the gas phase at pressures up to 1 MPa.

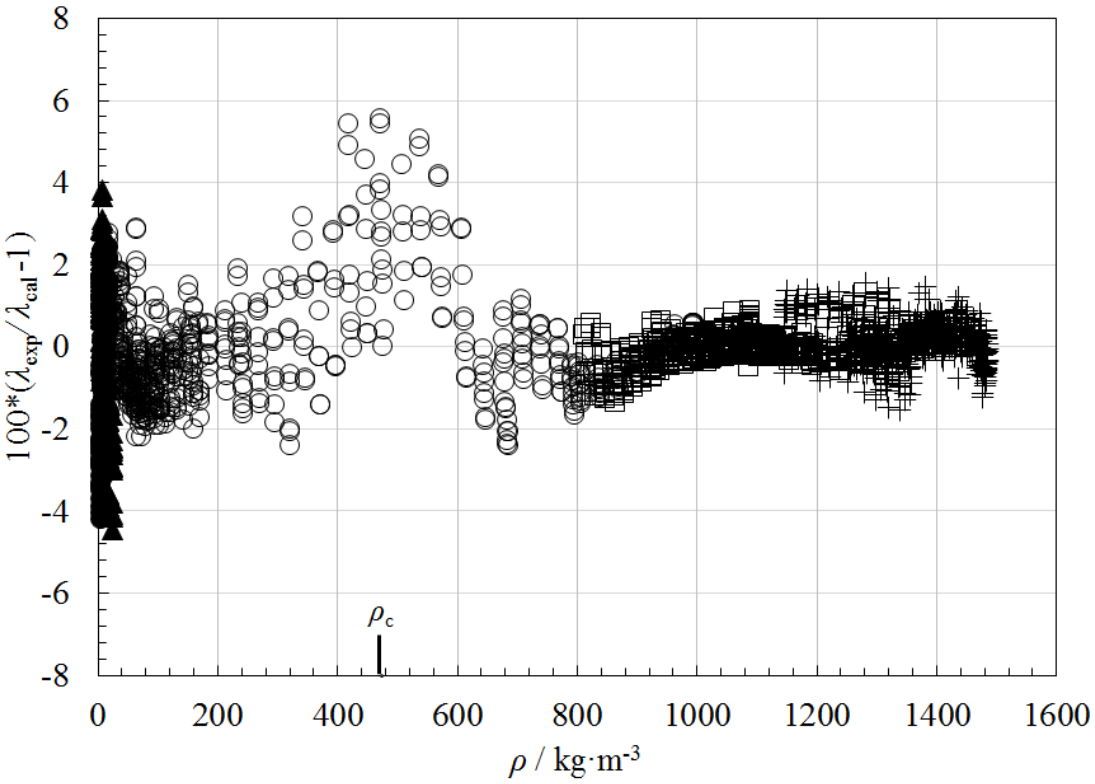

Figure 4. Relative deviation between the present experimental data and the correlation for the thermal conductivity of R1233zd(E) as a function of density: : ▲, double-wire transient vapor; ●, double-wire steady-state vapor; +, double-wire transient liquid; ○, single-wire transient vapor and supercritical; □, single-wire transient liquid.

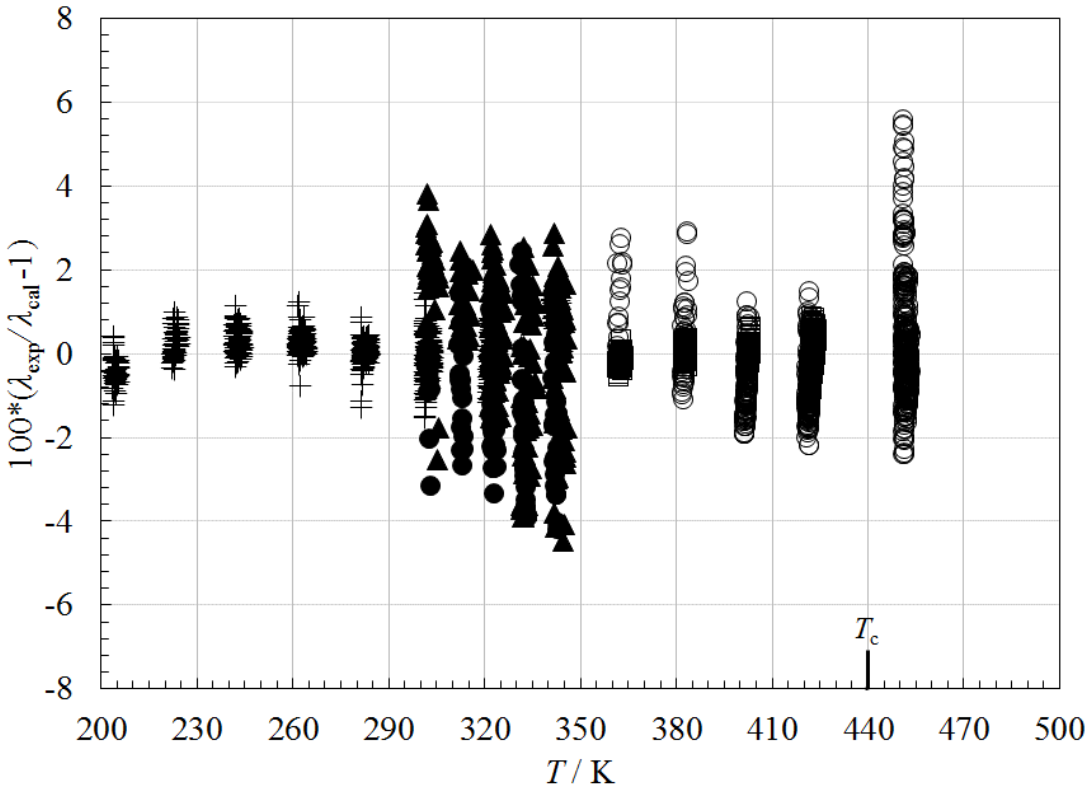

Figure 5. Relative deviation between the present experimental data and the correlation for the thermal conductivity of R1233zd(E) as a function of temperature: ▲, double-wire transient vapor; ●, double-wire steady-state vapor; +, double-wire transient liquid; ○, single-wire transient vapor and supercritical; □, single-wire transient liquid.

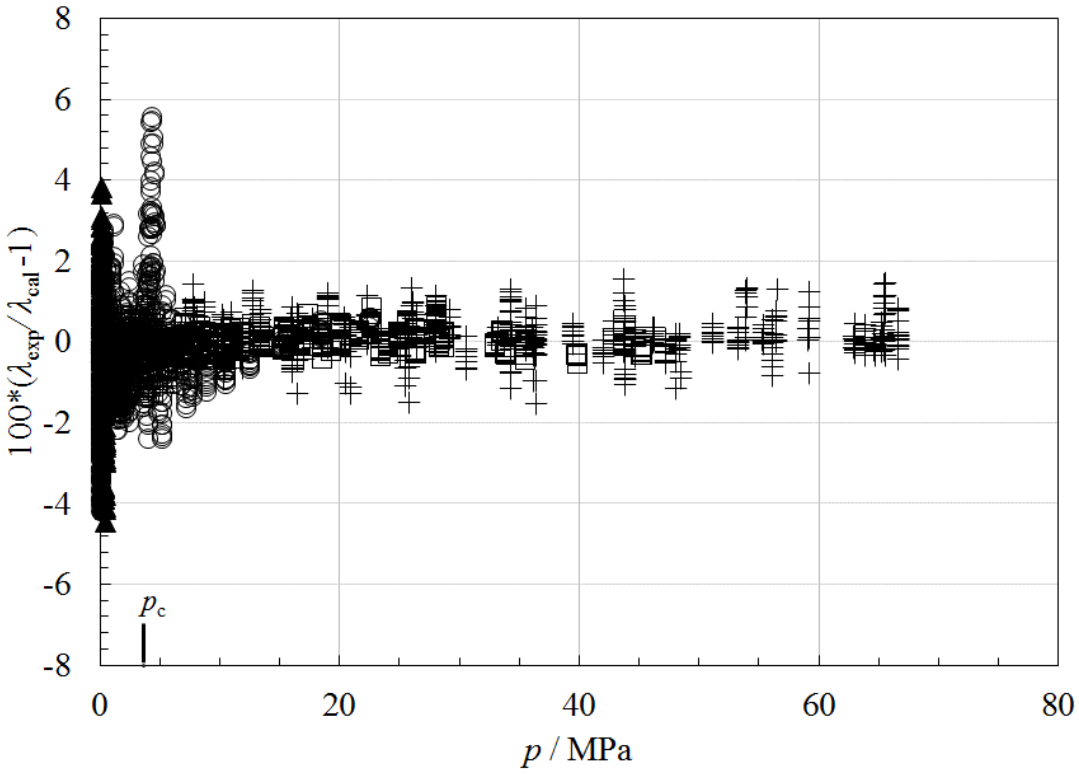

Figure 6. Relative deviation between the present experimental data and the correlation for the thermal conductivity of R1233zd(E) as a function of pressure: ▲, double-wire transient vapor; ●, double-wire steady-state vapor; +, double-wire transient liquid; ○, single-wire transient vapor and supercritical; □, single-wire transient liquid.

Table of Contents Graphic